

# Solibore-induced sediment resuspension in the Faeroe-Shetland Channel

Phil Hosegood, Jérôme Bonnin, and Hans van Haren

Royal Netherlands Institute of Sea Research (NIOZ), Den Burg, The Netherlands

Received 21 January 2004; accepted 31 March 2004; published 1 May 2004.

[1] High resolution measurements of temperature and current velocity over the seabed in the Faeroe-Shetland Channel (FSC) reveal an intense internal wave train, referred to as a solibore, propagating up the continental slope. In addition to enhancing turbulent mixing, a rotor formed at the leading edge of the solibore generates sediment fluxes  $O(10^2)$  greater than background levels. The interaction of solibores, which appear to evolve from baroclinic bores, with the seabed and the resulting rotor provides a dominant mechanism for the upward transport of sediment over continental slopes that may counteract downward avalanching of material by gravity. *INDEX TERMS:* 4211 Oceanography: General: Benthic boundary layers; 3022 Marine Geology and Geophysics: Marine sediments—processes and transport; 4568 Oceanography: Physical: Turbulence, diffusion, and mixing processes; 4512 Oceanography: Physical: Currents. **Citation:** Hosegood, P., J. Bonnin, and H. van Haren (2004), Solibore-induced sediment resuspension in the Faeroe-Shetland Channel, *Geophys. Res. Lett.*, 31, L09301, doi:10.1029/2004GL019544.

## 1. Introduction

[2] The hydrodynamics at continental slopes usually favour locally enhanced mixing [Munk and Wunsch, 1998], the suspension, deposition and transport of particulate matter [McCave *et al.*, 2001], and the supply of organic matter to the benthic community. At the slope, tidal flows and internal waves [e.g., Dickson and McCave, 1986; Cacchione *et al.*, 2002] may enhance currents periodically beyond the threshold required to suspend sediments, whilst the interaction between internal tides and upwelling/downwelling-favourable winds may either inhibit or promote cross-slope sediment transport [Xing and Davies, 2002]. Much shorter, particularly intense, events may erode the surface sediment layer altogether, exposing the underlying sediment and allowing the release of nutrients to the benthic boundary layer, stimulating the biological community [Otto and Balzer, 1998]. However, the temporal and spatial variability inherent to such features has meant that there has been a paucity of observations of sufficient detail to clarify their role in a geophysical context. Whilst recent shipborne observations from the Oregon shelf indicate a sequence of three turbulent internal solitary waves over a shoaling shelf [Klymak and Moum, 2003], the high-resolution observations from moored instruments we present here demonstrate the existence of a ‘solibore’ [Henry and Hoering, 1997] at the seabed in deep water over the

continental slope. A rotor, formed at its leading edge as previously suggested to occur [Thorpe, 1998] but not as yet observed, causes massive sediment resuspension which would indeed expose the underlying sediment.

[3] A solibore refers to an intense internal wave at a pycnocline which displays the properties of both a turbulent internal bore and a train of nonlinear internal solitary waves (ISW) or ‘solitons’. In a two-layer system where one layer is thicker than the other and the two are separated by a sharp density interface, the crests of the ISWs, as manifested by the vertical displacement of the interface, extend away from the thinner layer and into the thicker layer. For waves of elevation as observed here, where a thicker layer overlies a thinner layer, horizontal particle velocities are in the direction of propagation with upward velocities at the leading face with a return downward flow at the trailing edge. The term solibore was originally defined to describe the degeneration of internal tidal waves at pycnoclines near the sea surface [e.g., Sandstrom and Elliott, 1984; MacKinnon and Gregg, 2003] but similar features have also been observed in lakes arising from wind forced, internal seiches [Horn *et al.*, 2001]. In both cases they represent an important pathway for the transfer of energy from large to small scales where the energy may be dissipated during mixing processes. However, up to now near-bottom solibore-like features resulting from up-slope propagating baroclinic bores of high density water have only been observed in laboratory and numerical experiments on shoaling ISWs, just as nonlinear effects during the near-critical reflection of internal gravity waves from sloping bottoms also generate upslope propagating thermal fronts, associated with upslope currents and temperature drops. For sufficiently steep slopes or large wave amplitudes, the rear face of ISWs steepen due to nonlinear effects to form a bore which overturns because of kinematic instabilities (i.e., the particle velocity exceeds the speed of the bore face) [Vlasenko and Hutter, 2002], forming horizontal density intrusions in which are observed soliton-like waves of elevation, or ‘turbulent boluses’ [Helfrich, 1992]. Such boluses, or solitary waves with trapped cores, are potentially effective mechanisms for sediment transport. For less steep slopes or an incident ISW of smaller amplitude the ISW evolves to a dispersive wave tail.

## 2. Solibore Observations

[4] In 1999 an oceanographic survey was made along a transect perpendicular to the south-east slope of the FSC, north of Scotland (see inset of Figure 1). Data were obtained from moorings, deployed at the seabed and sampling

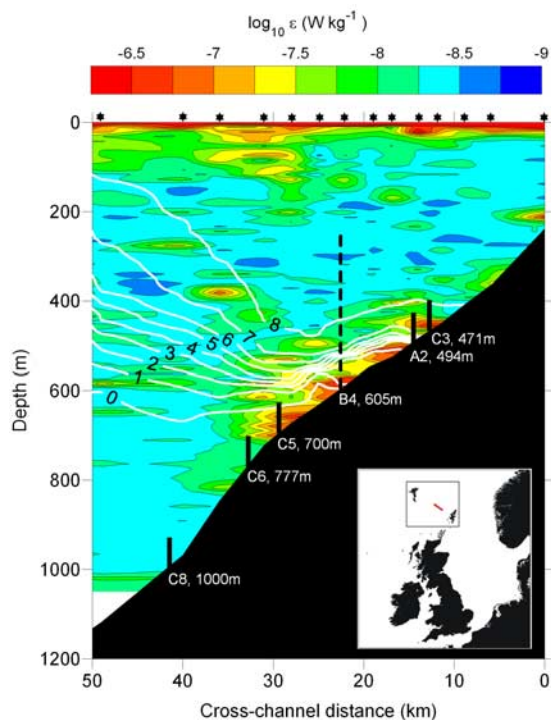


**Figure 1.** Temperature (indicated by isotherms in  $^{\circ}\text{C}$ ) and  $\varepsilon$  (measured using a free-falling microstructure probe exhibiting a noise level of  $10^{-9} \text{ W kg}^{-1}$ ) over the Shetland slope during the passage of the solibore on day 112. Mooring locations are indicated by the vertical black lines. On moorings C3, C5, C6 and C8 were mounted current meters and sediment traps at a height above the bottom,  $z$  of, 2, 30 m, whilst mooring B4 contained a 75 kHz Acoustic Doppler Current Profiler (ADCP). Mooring A2 consisted of a high resolution thermistor string and ADCP. The stars along the top x-axis represent the position where vertical profiles were conducted whilst the inset indicates the location (red line) of the transect.

primarily the bottom 50 m of the water column, and from vertical profiles of temperature  $T$  and velocity microstructure  $u'$  obtained during a transect across the slope at the time of the solibore. The relevant variables and their observation methods are given in the captions of Figures 1–4.

[5] An intrusion of cold water is observed, constrained to 50 m above the bottom (Figure 1). The intrusion is highly turbulent given the increased rates of dissipation of turbulent kinetic energy,  $\varepsilon$ , between depths of 700 m and 450 m. Values of  $\varepsilon$  rise from background values of  $10^{-9} \text{ W kg}^{-1}$  to  $\varepsilon > 10^{-7} \text{ W kg}^{-1}$  within the solibore. A measure of the amount of mixing occurring is given by the vertical eddy diffusivity,  $K_z = 0.2\varepsilon/N^2$  where  $N = [-(g/\rho_o)/(\Delta\rho/\Delta z)]^{0.5}$  is the buoyancy frequency,  $g$  is the acceleration due to gravity,  $\rho_o$  is a reference density and  $\Delta\rho/\Delta z$  is the change in density over 25 m vertical intervals. During the passage of the solibore  $K_z$  is consistently  $>10^{-4} \text{ m}^2 \text{ s}^{-1}$  within the bottom 30 m and reaches a maximum of  $K_z \approx 10^{-1} \text{ m}^2 \text{ s}^{-1}$  at 620 m. Thus  $K_z$  during the time of the event is consistently above the canonical value of  $10^{-4} \text{ m}^2 \text{ s}^{-1}$  proposed to be required to maintain the global thermohaline circulation [Munk and Wunsch, 1998] and the typically observed value of  $10^{-5} \text{ m}^2 \text{ s}^{-1}$  observed in the ocean away from topography.

Values of  $\varepsilon > 10^{-7} \text{ W kg}^{-1}$  are also observed near the surface and result from an atmospheric storm over the 2 days prior to the transect.

[6] On day 112 the solibore is observed as a strong temperature front at C3 (Figure 2a), the temperature dropping  $4.6^{\circ}\text{C}$  within one minute at  $z = 8 \text{ m}$ . At the same time, the cross-slope velocity,  $U$ , reverses from a down-slope to an up-slope direction (Figure 2b), whilst the long-slope current,  $V$ , increases strongly in the poleward direction at both C3 and C6 and remains in the poleward direction for more than 36 hours (Figure 2c). At C6 the poleward flow represents a distinct reversal from an equatorward direction.

[7] Sediment trap data indicate that sediment fluxes were massively enhanced on day 112 (Figure 3). The high sampling resolution of one day and near-bed location of the traps allows us to directly attribute this enhanced flux to the solibore. To allow sampling in high-energy environments [Gardner, 1985], all traps were modified to a cylindrical shape with an aspect ratio of 8 by adding a baffled (10 mm hexagons) PVC cylinder (1.5 m). Fluxes at C5 increase abruptly from  $O(1) \text{ g m}^{-2} \text{ d}^{-1}$  on day 111 to  $160 \text{ g m}^{-2} \text{ d}^{-1}$  on day 112, remaining high until day 116, whilst at C6 a maximum value of  $350 \text{ g m}^{-2} \text{ d}^{-1}$  occurs on day 113. The low fluxes at C3, with a mean value of  $0.2 \text{ g m}^{-2} \text{ d}^{-1}$ , are attributed to the bed material there being composed of hard consolidated sand, whilst at C8 where mean fluxes are  $5 \text{ g m}^{-2} \text{ d}^{-1}$ , the hydrodynamic regime is distinct from higher up the slope and thus not

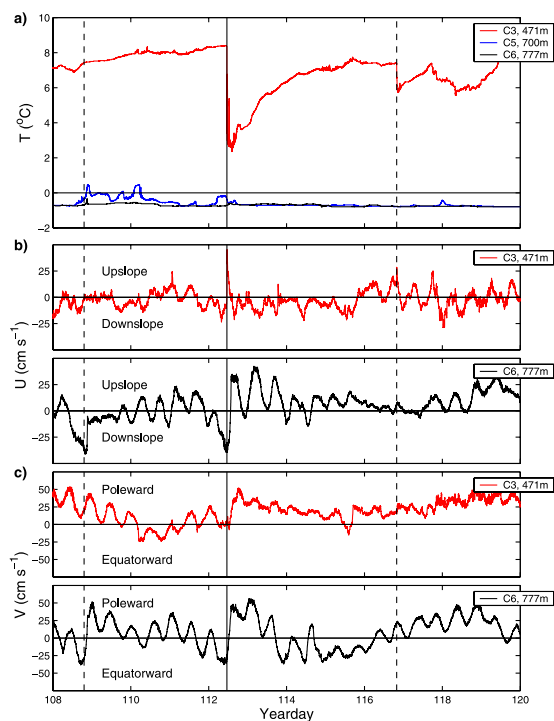


**Figure 2.** (a) Temperature, (b) cross-slope and (c) long-slope velocities observed at 8 m above the bottom. The solid vertical line corresponds to the temperature front at C3. The dashed lines correspond to a smaller but equally distinct drop in temperature on day 116, and a sudden current change at C6 on day 108.

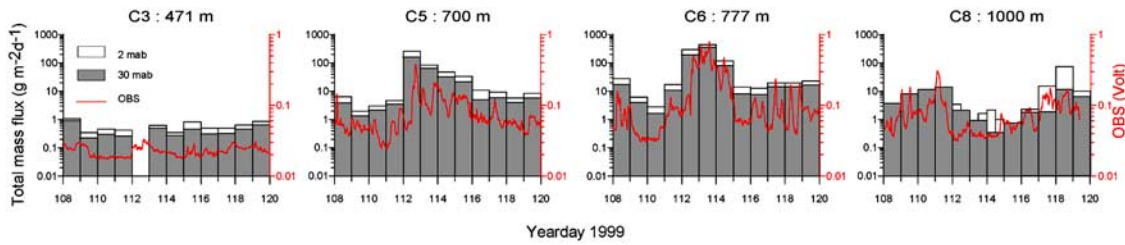


**Figure 3.** Sediment fluxes at 2 m (white bars) and 30 m (grey bars) above the bottom and optical backscatter sensor (OBS) data throughout deployment period. Tilt effect has been evaluated and shown to be minor [Bonnin *et al.*, 2002]. The OBS signal shows a good correlation with trap data and indicate that the large sediment fluxes are genuine and not due to trapping artefact.

subject to the same erosional processes. The resuspension potential of the event is evident from the greater proportion of large diameter particles ( $>100 \mu\text{m}$ ) found in the traps on day 112 at  $z = 30 \text{ m}$  at C6 as compared to the following 2 days when fluxes are composed of smaller particles. In conjunction with the one day time lag in maximum total mass flux between C5 on day 112 and that at C6, on day 113, this suggests the gradual down-slope settling out of the finer particles under the action of gravity following the initial resuspension and up-slope transport by the solibore.

[8] High resolution measurements over the bottom 30 m of the water column at A2 were enabled by the use of a fast sampling, accurate thermistor string [van Haren *et al.*, 2001] and a 600 kHz ADCP, each sampling once per minute and with a vertical resolution of 1 m and 0.5 m respectively. The resemblance of the intrusion to a solibore is clear as a bore-like face is followed by a wave train consisting of approximately 5 asymmetric waves extending into the thicker overlying layer (Figure 4a). The linear long wave phase speed,  $c_{linear} = [(g'H_1H_2)/(H_1 + H_2)]^{0.5}$ , where  $g' = g(\rho_2 - \rho_1)/\rho_2$  and  $\rho_1, \rho_2$  and  $H_1, H_2$  are upper and lower layer densities (calculated by establishing a temperature-salinity relationship from CTD-data) and thicknesses respectively, behind the bore is  $64 \pm 18 \text{ cm s}^{-1}$ . This exceeds the speed of the bore itself, determined as  $24 \text{ cm s}^{-1}$  by the time of arrival of the temperature front at A2 and C3, and is one of the properties which characterises bores [Henyey and Hoering, 1997]. The temperature and velocity fields are consistent with the results of numerical models on the overturning of a bore resulting from a shoaling ISW [Vlasenko and Hutter, 2002]. Cross-slope velocities easily exceed  $24 \text{ cm s}^{-1}$  towards the front of the solibore with a maximum of  $52 \text{ cm s}^{-1}$  observed at  $z = 16 \text{ m}$ , satisfying the kinematic instability mechanism required for overturning. Superimposed on the large-scale shape of the solibore are smaller scale particle velocities related to upslope propagating internal solitary waves (Figures 4b and 4c). Vertical velocities are directed upwards at the leading edges and downwards on the trailing edges of the individual waves, as expected for ISWs of elevation. However, the profiles of the waves are not of the  $\text{sech}^2$  shape expected for ISWs; thus we propose that the waves are in fact turbulent boluses resulting from an overturned bore. At the leading edge of the solibore a rotor, proposed to occur when internal waves break on a slope [Thorpe, 1998], is formed. Flow is contrary to the forward overturning of surface waves on a beach, with upwards

velocities, of maximum amplitude  $16.2 \text{ cm s}^{-1}$ , leading the downward flow, of maximum amplitude  $14 \text{ cm s}^{-1}$ .

[9] The rotor enables the greatly enhanced sediment fluxes observed, especially higher above the bed at  $z = 30 \text{ m}$  to where the enhanced vertical velocity extends. Following resuspension by the rotor, the turbulent boluses transport the sediment up the slope. Large bottom-stresses

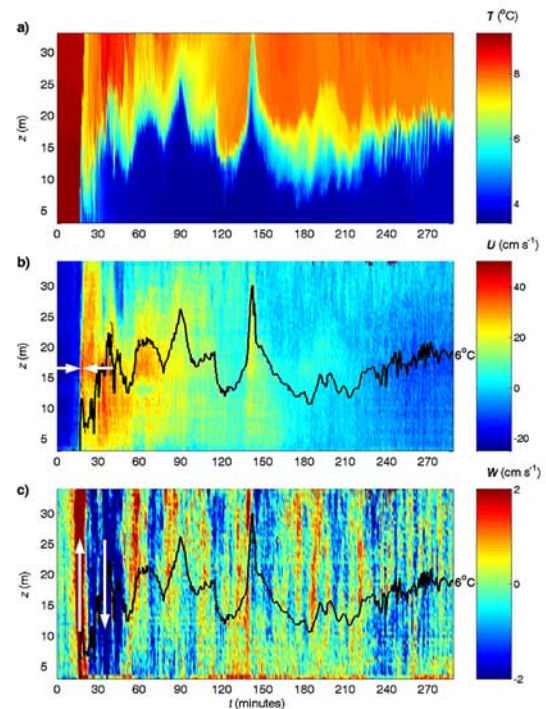


**Figure 4.** High resolution (a) temperature, (b) cross-slope and (c) vertical velocities during the passage of the solibore on day 112 at A2. The time axis is referenced arbitrarily to  $t = 0$  at  $\sim 15$  minutes before the arrival of the leading edge (LE) of the solibore. The along-slope velocity component is negligible during the solibore and thus omitted. The LE is followed by a train of 5 soliton-like waves of elevation, with amplitudes,  $\eta$ , and wavelengths,  $L$  (calculated at  $0.42\eta$ ), of  $O(10 \text{ m})$  and  $\sim 200 \text{ m}$  respectively, and a packet of high frequency waves at  $t = 240\text{--}270$  minutes with periods near the local buoyancy period  $\approx 5$  minutes. White arrows indicate the horizontally convergent currents at LE in (b) and, in (c), the rotor of vertical velocities.

were observed at other times during the experiment but with no enhanced fluxes, implying that the dominant sediment transport mechanism is not simply the exceedance of a bottom-stress threshold. Whilst sediment transport is concentrated at depths of 500–800 m, confirmed by the lack of significantly enhanced fluxes at C3, the echo intensity from the ADCP at A2 indicates that the little sediment that is held in suspension by the solibore is found towards the leading face where the rotor is observed. The upslope transport of sediment by the solibore is contrary to the usually assumed downslope sediment pathways from shelf seas to the abyss. The size of particles resuspended by the solibore indicates the erosion of the surface layer, enabling the exposure of the underlying sediments to the water column and the release of dissolved organic carbon and nutrients. Thus the degree of resuspension attributed to the solibore is important for the observed zonation of the benthic biological community.

### 3. Discussion

[10] The temperature and velocity signals observed at C3 and C6 both prior to and after day 112 indicate an approximately 4 day periodicity associated with the forcing for the solibores (Figure 1). A subinertial variability is further suggested by data from instruments deployed for 4 months following the current deployment period. Such a periodicity is not consistent with semidiurnal tidal forcing, nor is the abrupt reversal in the long-slope current component associated with passage of the solibore and the ensuing sustained surge in the poleward direction. The solibore also appeared during a barotropic neap tide when internal tidal forcing would be expected to be weakest. Bottom trapped topographic Rossby waves [Rhines, 1970] were considered as a forcing mechanism as the ADCP at B4 indicated bottom intensified currents during the solibore. However, the bottom intensified motion was merely due to the strong currents being constrained to the fluid below the thermocline, the position of which moves upwards past the mooring throughout the duration of the solibore. At this time the cause of the 4-day quasi periodicity remains obscure, but the passage of low pressure systems through the region two days prior to each of the three events on days 108, 112 and 116 suggest that atmospheric forcing may be responsible. As the sediment fluxes appear to result from the sudden passage of the solibore rather than due to persistent winds during the preceding storm [Xing and Davies, 2002] future work aims to establish the possibility of Kelvin waves evolving nonlinearly to cause rapid perturbations in the thermocline, in the same way as observed in Lake Geneva [Thorpe et al., 1996], and which may then form near-bed solibores.

### 4. Conclusions

[11] We have shown that high resolution measurements made near the seabed over the continental slope reveal the presence of a solibore propagating up the slope and facilitating massive sediment resuspension due to the formation of a rotor at its leading edge. Grain size analysis shows that the enhanced resuspension of large particles permits the exposure of the underlying sediments, promoting biological

growth. Despite their limited impact on deep ocean mixing due to their relatively infrequent occurrence, our measurements indicate not only the importance of solibores as a means of sediment transport, but also their evolution from a baroclinic bore, potentially generated by meteorological forcing.

[12] **Acknowledgments.** “PROCS” was funded by the Netherlands Organisation for the Advancement of Scientific Research (NWO). We thank Kees Veth for obtaining the microstructure data and Theo Hillebrand for the preparation of moored instruments. Sjeff Zimmerman reviewed an earlier draft of the paper.

### References

- Bonnin, J., W. van Raaphorst, G.-J. Brummer, H. van Haren, and H. Malschaert (2002), Intense mid-slope resuspension of particulate matter in the Faeroe-Shetland Channel: Short-term deployment of near-bottom sediment traps, *Deep Sea Res., Part I*, 49, 1485–1505.
- Cacchione, D. A., L. F. Pratson, and A. S. Ogston (2002), The shaping of continental slopes by internal tides, *Science*, 296, 724–727.
- Dickson, R. R., and I. N. McCave (1986), Nepheloid layers on the continental slope west of Porcupine Bank, *Deep Sea Res., Part A*, 33, 791–818.
- Gardner, W. D. (1985), The effect of tilt on sediment trap efficiency, *Deep Sea Res.*, 32, 349–362.
- Helfrich, K. R. (1992), Internal solitary wave breaking and run-up on a uniform slope, *J. Fluid Mech.*, 243, 133–154.
- Henry, F. S., and A. Hoering (1997), Energetics of borelike internal waves, *J. Geophys. Res.*, 102, 3323–3330.
- Horn, D. A., J. Imberger, and G. N. Ivey (2001), The degeneration of large-scale interfacial gravity waves in lakes, *J. Fluid Mech.*, 434, 181–207.
- Klymak, J. M., and J. M. Moum (2003), Internal solitary waves of elevation advancing on a shoaling shelf, *Geophys. Res. Lett.*, 30(20), 2045, doi:10.1029/2003GL017706.
- MacKinnon, J. A., and M. C. Gregg (2003), Mixing on the late-summer New England shelf—Solibores, shear, and stratification, *J. Phys. Oceanogr.*, 33, 1476–1492.
- McCave, I. N., I. R. Hall, A. N. Antia, L. Chou, F. Dehairs, R. S. Lampitt, L. Thomsen, T. C. E. van Weering, and R. Wollast (2001), Sources, composition and flux of suspended particulate material on the European margin 47°–50°N: A synthesis of results from the OMEX I programme, *Deep Sea Res., Part II*, 48, 3107–3139.
- Munk, W., and C. Wunsch (1998), Abyssal recipes II: Energetics of tidal and wind mixing, *Deep Sea Res.*, 45, 1977–2010.
- Otto, S., and W. Balzer (1998), Release of dissolved organic carbon (DOC) from sediments of the N. W. European continental margin (Goban Spur) and its significance for benthic carbon cycling, *Prog. Oceanogr.*, 42, 127–144.
- Rhines, P. (1970), Edge-, bottom-, and Rossby waves in a rotating stratified fluid, *Geophys. Fluid Dyn.*, 1, 273–302.
- Sandstrom, H., and J. A. Elliott (1984), Internal tide and solitons on the Scotian Shelf: A nutrient pump at work, *J. Geophys. Res.*, 89, 6415–6426.
- Thorpe, S. A. (1998), Some dynamical effects of internal waves and the sloping sides of lakes, in *Physical Processes in Lakes and Oceans, Coastal Estuarine Stud.*, vol. 54, edited by J. Imberger, pp. 441–460, AGU, Washington, D. C.
- Thorpe, S. A., J. M. Keen, R. Jiang, and U. Lemmin (1996), High frequency internal waves in Lake Geneva, *Philos. Trans. R. Soc. London, Ser. A*, 354, 237–257.
- van Haren, H., R. Groenewegen, M. Laan, and B. Koster (2001), A fast and accurate thermistor string, *J. Atmos. Oceanic Technol.*, 18, 256–265.
- Vlasenko, V., and K. Hutter (2002), Numerical experiments on the breaking of solitary internal waves over a slope-shelf topography, *J. Phys. Oceanogr.*, 32, 1779–1793.
- Xing, J., and A. M. Davies (2002), Influence of wind direction, wind waves, and density stratification upon sediment transport in shelf edge regions: The Iberian shelf, *J. Geophys. Res.*, 107(C8), 3101, doi:10.1029/2001JC000961.

P. Hosegood, J. Bonnin, and H. van Haren, Royal Netherlands Institute of Sea Research (NIOZ), P.O. Box 59, Den Burg, Texel 1790AB, The Netherlands. (hosegood@nioz.nl)